

7-1979

Direct relation between Fresnel's interface reflection coefficients for the parallel and perpendicular polarizations

R. M.A. Azzam

University of New Orleans, razzam@uno.edu

Follow this and additional works at: https://scholarworks.uno.edu/ee_facpubs



Part of the [Electrical and Electronics Commons](#), and the [Physics Commons](#)

Recommended Citation

R. M. A. Azzam, "Direct relation between Fresnel's interface reflection coefficients for the parallel and perpendicular polarizations," *J. Opt. Soc. Am.* 69, 1007-1016 (1979)

This Article is brought to you for free and open access by the Department of Electrical Engineering at ScholarWorks@UNO. It has been accepted for inclusion in Electrical Engineering Faculty Publications by an authorized administrator of ScholarWorks@UNO. For more information, please contact scholarworks@uno.edu.

Direct relation between Fresnel's interface reflection coefficients for the parallel and perpendicular polarizations

R. M. A. Azzam

Department of Electrical Engineering, School of Engineering, University of New Orleans, Lakefront, New Orleans, Louisiana 70122

(Received 11 December 1978)

We have found a significant relation, $r_p = r_s(r_s - \cos 2\phi)/(1 - r_s \cos 2\phi)$, between Fresnel's interface complex-amplitude reflection coefficients r_p and r_s for the parallel (p) and perpendicular (s) polarizations at the same angle of incidence ϕ . This relation is universal in that it applies to reflection at all interfaces between homogeneous isotropic media collectively and, of course, throughout the electromagnetic spectrum. We investigate the properties of this function, $r_p = f(r_s)$, and its inverse, $r_s = g(r_p)$, as conformal mappings between the complex planes of r_s and r_p . A related function, $\rho = (r_s - \cos 2\phi)/(1 - r_s \cos 2\phi)$, which is a bilinear transformation, is also studied, where $\rho = r_p/r_s$ is the (ellipsometric) ratio of reflection coefficients. Several previously described reflection characteristics come out readily as specific results of this work. Simple explicit analytical and graphical solutions are provided to determine reflection phase shifts and the dielectric function from measured p and s reflectances at the same angle of incidence. We also show that when r_p is real, negative, and in the range $-1 \leq r_p \leq -\tan^2(\phi - 45^\circ)$, r_s is complex and its locus in the complex plane is an arc of a circle with center on the real axis at $\sec 2\phi$ and radius of $|\tan 2\phi|$. Under these conditions, we also find the interesting result that $|r_s| = |r_p|^{1/2}$.

I. INTRODUCTION

The reflection of a monochromatic electromagnetic plane wave at the planar interface between two linear homogeneous and isotropic media is governed by the well-known Fresnel coefficients. For the two linear polarizations parallel (p or TM) and perpendicular (s or TE) to the plane of incidence, these coefficients are given by¹

$$r_p = \frac{\epsilon \cos \phi - (\epsilon - \sin^2 \phi)^{1/2}}{\epsilon \cos \phi + (\epsilon - \sin^2 \phi)^{1/2}}, \quad (1)$$

$$r_s = \frac{\cos \phi - (\epsilon - \sin^2 \phi)^{1/2}}{\cos \phi + (\epsilon - \sin^2 \phi)^{1/2}}, \quad (2)$$

where ϕ is the angle of incidence and ϵ is the ratio of the dielectric function of the medium of refraction to that of the medium of incidence. We assume the $e^{j\omega t}$ time dependence and p and s directions as in the Nebraska (Muller) conventions.²

In this paper we find a direct relation between r_p and r_s at the same angle of incidence ϕ , study its properties, and give one of its applications. This complements earlier work on the transformation of the Fresnel coefficients between normal and oblique incidence.³

II. RELATION BETWEEN r_p AND r_s

To relate r_p and r_s we eliminate ϵ between Eqs. (1) and (2). In terms of

$$x = (\epsilon - \sin^2 \phi)^{1/2}, \quad (3)$$

Eqs. (1) and (2) become

$$r_p = \frac{\cos \phi (x^2 + \sin^2 \phi) - x}{\cos \phi (x^2 + \sin^2 \phi) + x}, \quad (4)$$

$$r_s = (\cos \phi - x)/(\cos \phi + x). \quad (5)$$

From Eq. (5), $x = \cos \phi(1 - r_s)/(1 + r_s)$, which we substitute into Eq. (4) to obtain

$$r_p = r_s(r_s - \cos 2\phi)/(1 - r_s \cos 2\phi). \quad (6)$$

Equation (6) is the desired direct relation between Fresnel's interface complex-amplitude reflection coefficients r_p and r_s for the p and s polarizations at the same angle of incidence⁴ ϕ . Significantly, this relation is independent of the two media that define the interface and applies, of course, throughout the entire electromagnetic spectrum. Although Eqs. (1) and (2), hence Eq. (6), are valid generally when both media are absorbing and ϕ is complex, we will assume hereafter that the medium of incidence is transparent and that ϕ is real.

At normal incidence, $\phi = 0$, and at grazing incidence, $\phi = 90^\circ$, Eq. (6) reduces to $r_p = -r_s$ and $r_p = r_s$ respectively, as expected. When $\phi = 45^\circ$, Eq. (6) reduces to $r_p = r_s^2$, a result which is also known to be true for this special case.^{5,6,7}

Equation (6) predicts Brewster's condition, namely that r_p can become zero; this occurs when

$$r_s = \cos 2\phi, \quad (7)$$

which is a simple expression for the nonzero reflection coefficient for the s polarization at the Brewster angle ($\phi = \phi_B$).

The partial derivative of Eq. (6) with respect to r_s ,

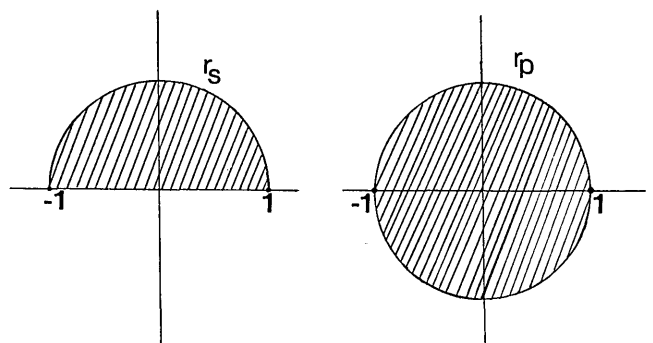


FIG. 1. Domains of all permissible values of Fresnel's interface reflection coefficients r_s (left) and r_p (right) for the s and p polarizations.

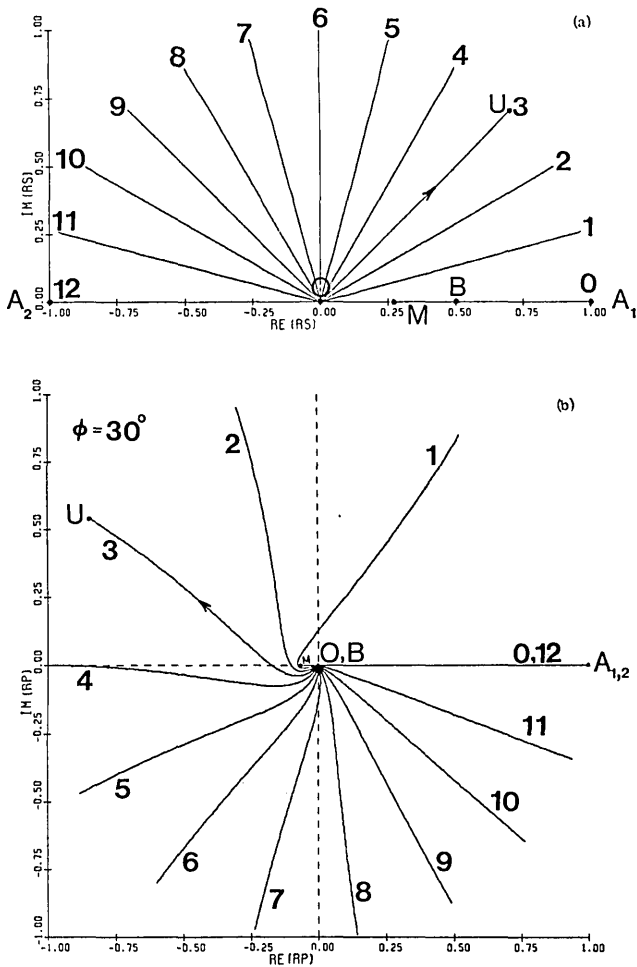


FIG. 2. Mapping of r_s onto r_p according to the complex analytic function $r_p = r_s(r_s - \cos 2\phi)/(1 - r_s \cos 2\phi)$ when $\phi = 30^\circ$. The angularly equispaced straight lines through the origin 0, 1, 2, . . . , 12 in the r_s plane represent lines of equal reflection phase shift for the s polarization, $\delta_s = \arg r_s = 0, 15^\circ, 30^\circ, \dots, 180^\circ$ respectively and their images in the r_p plane are marked by the same numbers. Points that are images of one another are also marked by the same letters. (This notation applies to the following figures as well.) As r_s scans straight line 3, for example, from the origin O to U on the unit circle in the r_s plane, r_p scans curve 3 from the origin O to U on the unit circle in the r_p plane, in the direction of the indicated arrows.

$$\frac{\partial r_p}{\partial r_s} = (-r_s^2 \cos 2\phi + 2r_s - \cos 2\phi)/(1 - r_s \cos 2\phi)^2 \quad (8)$$

vanishes when⁸

$$r_s = \sec 2\phi - \tan 2\phi = -\tan(\phi - 45^\circ). \quad (9)$$

Substitution of this value of r_s into Eq. (6) gives

$$r_p = -(\sec 2\phi - \tan 2\phi)^2 = -\tan^2(\phi - 45^\circ) = -r_s^2. \quad (10)$$

The reader can verify that Eqs. (9) and (10) give the Fresnel coefficients for reflection at interfaces between transparent media such that the angle of refraction is 45° . Because $\partial r_p / \partial r_s = (\partial r_p / \partial \epsilon)(\partial \epsilon / \partial r_s)$, it follows that $\partial r_p / \partial \epsilon = \partial r_p / \partial \nu = 0$, where $\epsilon = \nu^2$ and ν is the complex relative refractive index. This result is in agreement with what we have found before in Ref. 9.

In the following section we investigate Eq. (6) more fully

as a conformal mapping¹⁰ between the complex planes of r_s and r_p .¹¹

III. MAPPING OF r_s ONTO r_p

In the Nebraska (Muller) conventions,² r_s is restricted to the inside and boundaries of the upper-half of the unit circle in the complex r_s plane, and, consequently from Eq. (6), r_p is limited to the interior and boundary of the full unit circle in the complex r_p plane, Fig. 1. For every value of r_s only one value of r_p is obtained from Eq. (6), but not vice versa. There is one-to-one correspondence between points in the domains of all permissible values of r_s and r_p shown in Fig. 1 except for points along the real axis.

Figure 2 shows mapping by the complex analytic function $r_p = f(r_s)$ of Eq. (6) of angularly equispaced straight lines through the origin of the r_s plane (lines of equal reflection phase shift for the s polarization $\delta_s = \arg r_s = 0, 15^\circ, 30^\circ, \dots$,

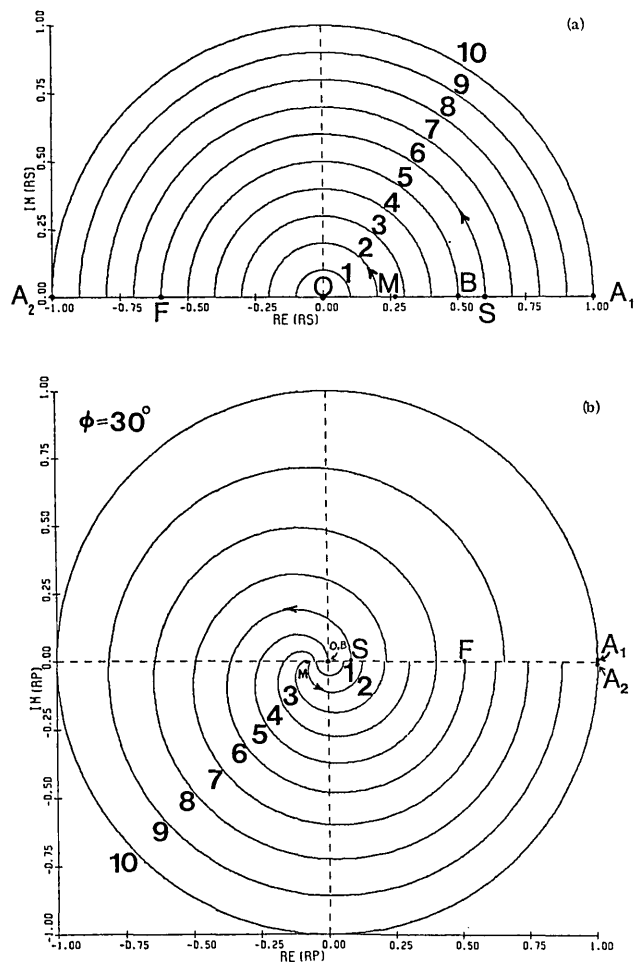


FIG. 3. Mapping of r_s onto r_p according to the complex analytic function $r_p = r_s(r_s - \cos 2\phi)/(1 - r_s \cos 2\phi)$ when $\phi = 30^\circ$. The equispaced semicircles centered on the origin 1, 2, 3, . . . , 10 in the r_s plane represent lines of equal amplitude reflectance for the s polarization, $|r_s| = 0.1, 0.2, 0.3, \dots, 1.0$ respectively and their images in the r_p plane are marked by the same numbers. The images in the r_p plane of semicircles 1, 2 lie entirely below the real axis, while the images of semicircles 3 to 10 are one-full-revolution spirals. As r_s traces semicircle 6, for example, from S to F in the r_s plane, r_p traces spiral 6 from S to F in the r_p plane, in the direction of the indicated arrows.

180°) onto the r_p plane, for an angle of incidence $\phi = 30^\circ$. Here, and in other figures, lines and points that are images of one another are marked by the same numbers and letters respectively, and arrows indicate directions in which lines are traced. Mapping of points along the real axis of the r_s plane onto the r_p plane requires special attention. Such points represent reflection of electromagnetic radiation at interfaces between transparent media. When r_s moves along the positive real axis from the origin $O(r_s = 0)$ to $M(r_s = -\tan(\phi - 45^\circ) = 0.268)$ to $B(r_s = \cos 2\phi = 0.5)$, r_p moves along the negative real axis from $O(r_p = 0)$ to $M(r_p = -\tan^2(\phi - 45^\circ) = -0.072)$

and back to B which coincides with the origin O . The reversal of the direction of motion of r_p at the point M is consistent with the fact that $\partial r_p / \partial r_s = 0$ at that point [see the discussion associated with Eqs. (9) and (10)]. M represents refraction at 45° while B represents reflection at the Brewster angle at interfaces between transparent media. If r_s moves from B to $A_1(r_s = 1)$, or from O to $A_2(r_s = -1)$, r_p moves from O to $A_{1,2}(r_p = 1)$. It is evident that two values of r_s produce the same value of r_p .

Figure 3 shows how a family of equispaced semicircles

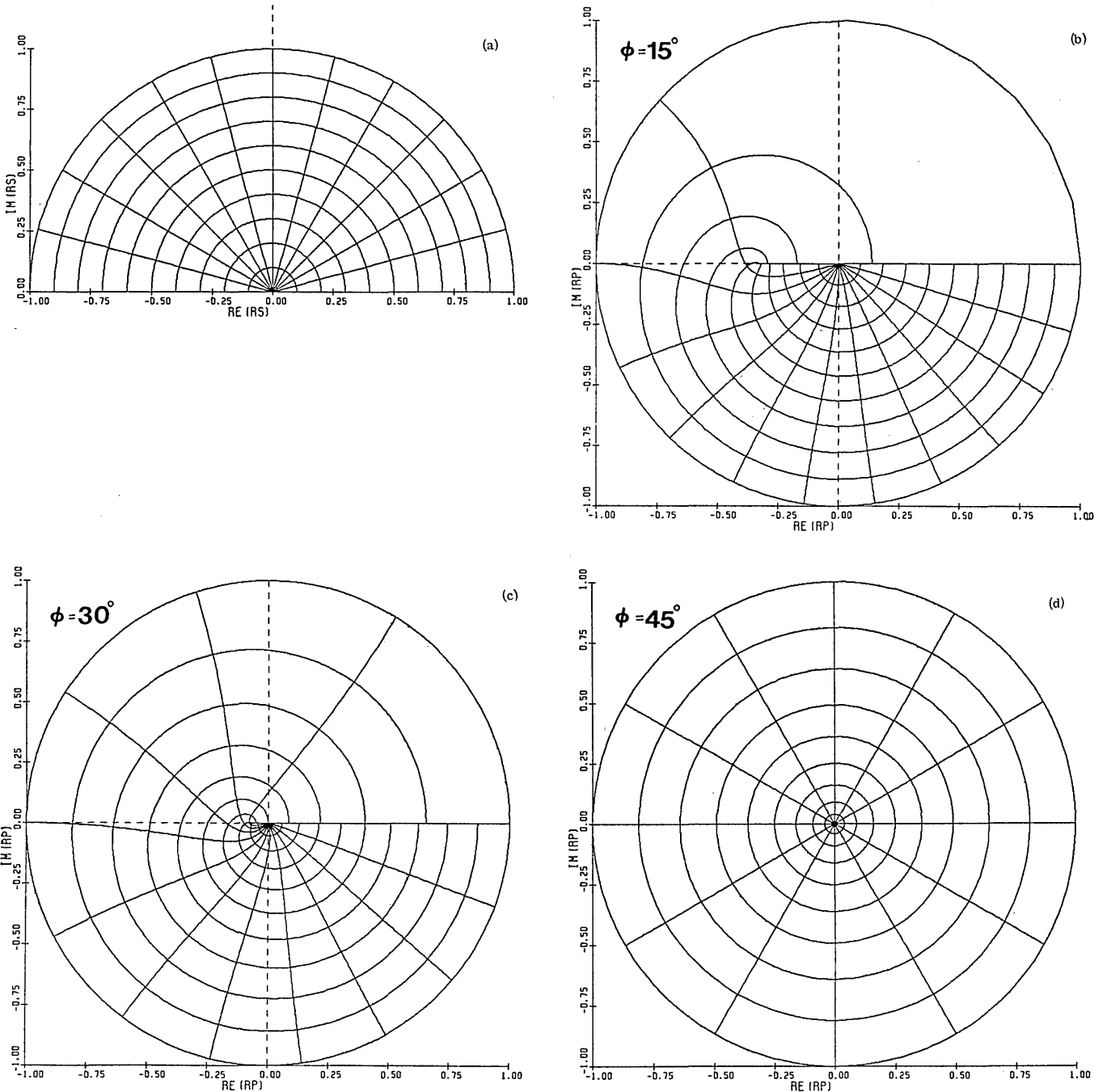


FIG. 4. Mapping of r_s onto r_p according to the complex analytic function $r_p = r_s(r_s - \cos 2\phi)/(1 - r_s \cos 2\phi)$ when $\phi = 15^\circ, 30^\circ, 45^\circ, 60^\circ, 75^\circ$. The orthogonal families of straight lines and semicircles through and around the origin in the r_s plane are mapped onto orthogonal sets of curves in the r_p plane. The orthogonal sets that correspond to $\phi = 30^\circ$ are obtained from the superposition of Figs. 2 and 3. To identify individual curves use Figs. 2 and 3 as a guide. (Continued on p. 1010.)

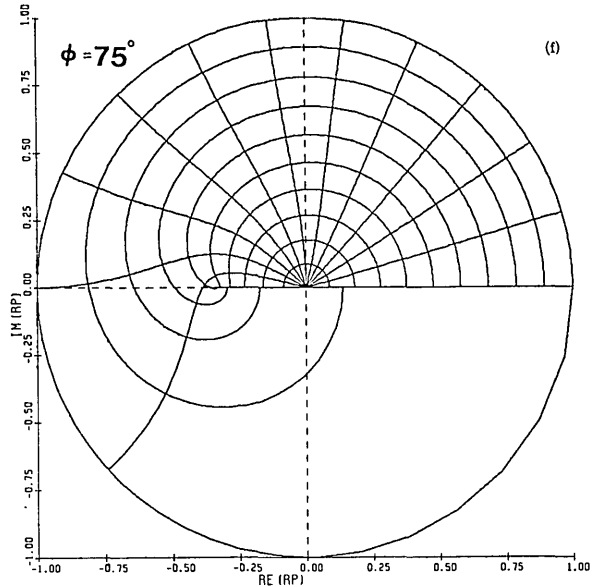
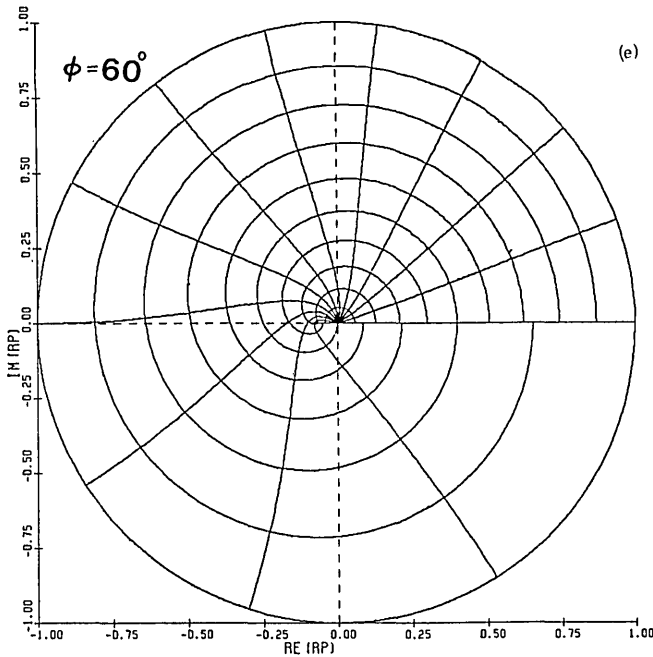


FIG. 4. (continued).

centered on the origin in the r_s plane (lines of equal amplitude reflectance for the s polarization $|r_s| = 0.1, 0.2, 0.3, \dots, 1.0$) are mapped by Eq. (6) onto the r_p plane, at the same angle of incidence $\phi = 30^\circ$ as in Fig. 2. Semicircles 1 and 2 have images that lie entirely below the real axis of the r_p plane. We can show that this actually applies to all semicircles with radii $|r_s| \leq OM = |\tan(\phi - 45^\circ)| = 0.268$. Semicircles 3 to 10, for which $|r_s| > |\tan(\phi - 45^\circ)|$, have images in the r_p plane that are one-full-revolution spirals. The spiralling takes place around the point M .

The superposition of Figs. 2 and 3 produces orthogonal families of curves in the r_s and r_p planes. This is shown in Fig. 4 for five angles of incidence including 30° ($\phi = 15^\circ, 30^\circ, 45^\circ, 60^\circ, 75^\circ$). Orthogonal sets of curves for $\phi = 45^\circ + \theta$ and $\phi = 45^\circ - \theta$ are mirror images of one another with respect to the real axis. Figure 4 gives as complete a picture of the mapping properties of Eq. (6) as is graphically possible. It provides useful nomograms that can be used to obtain quick estimates of the complex reflection coefficient r_p for given values of r_s , by locating in the r_p plane the point of intersection of the two contours representing $|r_s| = \text{constant}$ and $\text{arg} r_s = \text{constant}$.

IV. INVERSE TRANSFORMATION: MAPPING OF r_p ONTO r_s

Equation (6) can be inverted easily to give r_s as a function of r_p :

$$r_s = \frac{1}{2} \cos 2\phi (1 - r_p) + \left(r_p + \frac{1}{4} \cos^2 2\phi (1 - r_p)^2 \right)^{1/2}. \quad (11)$$

The inverse function, $r_s = g(r_p)$, Eq. (11), is double-valued; for every r_p there are two values of r_s that correspond to the two values of the square root. However, because r_s is limited to the upper-half of the unit circle, values of r_s with negative

imaginary parts are rejected. It follows that Eq. (11) gives two physically acceptable values of r_s only if r_p is real.

Figure 5 shows mapping by the complex analytic function $r_s = g(r_p)$ of Eq. (11) of angularly equispaced straight lines through the origin of the r_p plane (lines of equal reflection phase shift for the p polarization $\delta_p = \text{arg} r_p = 0, 15^\circ, 30^\circ, \dots, 345^\circ$) onto the r_s plane when the angle of incidence $\phi = 30^\circ$. The origin $r_p = 0$ represents two physically distinguishable situations: (i) Reflection from interfaces in the limit when the two media on opposite sides of the interface become the same; in this case, we also have $r_s = 0$, and the situation is represented by the point O . (ii) Reflection at the Brewster angle in which case $r_s = \cos 2\phi$, and this instance is represented by the point B . Thus the origin of the r_p plane has two separate image points in the r_s plane one is $O(r_s = 0)$ and the other is $B(r_s = \cos 2\phi)$. When r_p moves along the positive real axis of the r_p plane from the origin to A_1 its two distinct images in the r_s plane move in opposite directions along the segments of the real axis from B to A_1 ($r_s = 1$) and from O to A_1 ($r_s = -1$). If r_p moves along the negative real axis of the r_p plane from the origin to M ($r_p = -\tan(\phi - 45^\circ) = -0.072$) its two images in the r_s plane move in opposite directions on the segments of the real axis from B to M ($r_s = -\tan(\phi - 45^\circ) = 0.268$) and from O to M . Further movement of r_p along the negative real axis of the r_p plane from M to A_2 generates the curve MA_2 in the r_s plane. The interesting conclusion follows immediately that the reflection coefficient of the p polarization can become real and negative while, at the same time, the reflection coefficient for the s polarization is complex. This result, which is readily obtained from the present study, was recently arrived at in a different way.¹² In the appendix, we prove that the curve MA_2 in Fig. 5 is in fact an arc of a circle with center on the real axis at $\sec 2\phi$ and radius of $|\tan 2\phi|$. This appendix gives other new information that supplements the results of Ref. 12.

In Fig. 5, straight lines that start from the origin and ter-

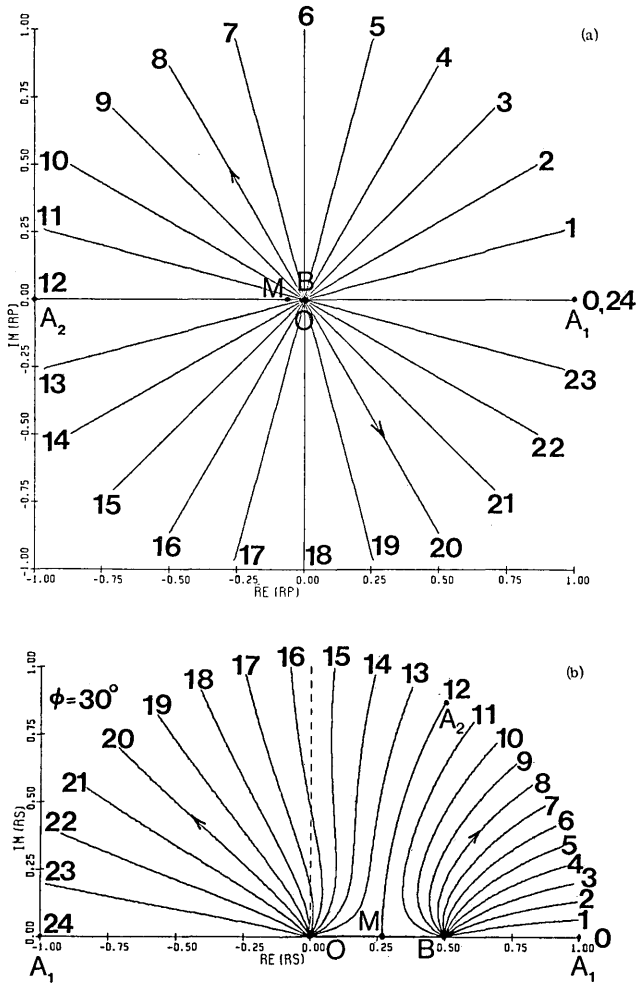


FIG. 5. Inverse mapping of r_p onto r_s according to the complex analytic function $r_s = (1/2) \cos 2\phi(1 - r_p) + [r_p + (1/4) \cos^2 2\phi(1 - r_p)^2]^{1/2}$ when $\phi = 30^\circ$. The angularly equispaced straight lines through the origin 0, 1, 2, ..., 23 in the r_p plane represent lines of equal reflection phase shift for the p polarization, $\delta_p = \arg r_p = 0, 15^\circ, 30^\circ, \dots, 345^\circ$ respectively and their images in the r_s plane are marked by the same numbers. The images in the r_s plane of straight lines, 1, 2, ..., 11 in the upper half of the r_p plane all originate from the point B ($r_s = \cos 2\phi = 0.5$), while the images of straight lines 13, 14, ..., 23 in the lower half of the r_p plane all pass through the origin O . The segment MA_2 of the negative real axis of the r_p plane is imaged onto circle arc MA_2 in the r_s plane. MA_2 divides the upper half of the unit circle in the r_s plane into two domains, one to its right and the other to its left, that correspond to the upper and lower halves of the unit circle in the r_p plane respectively.

minate on the unit circle in the upper half of the r_p plane ($0 < \arg r_p < 180^\circ$) are mapped onto curves that all originate from the same point B and terminate on (the arc $A_1 A_2$ of) the unit circle in the r_s plane. The remaining straight lines through the origin in the lower half of the r_p plane ($180^\circ < \arg r_p < 360^\circ$) are mapped onto a separate set of curves that originate from the point O and terminate on (the arc $A_2 A_1$ of) the unit circle in the r_s plane. Thus the upper and lower halves of the unit circle in the r_p plane are mapped onto the subdomains of the upper half of the unit circle in the r_s plane to the right and to the left, respectively, of the circle arc MA_2 .

Figure 6 shows how a family of circles centered on the origin in the r_p plane (lines of equal amplitude reflectance for the

p polarization, $|r_p| = 0.1, 0.2, \dots, 1.0$) are mapped by Eq. (11) onto the r_s plane.

The superposition of Figs. 5 and 6 produces orthogonal sets of curves in the r_p and r_s planes. This is shown in Fig. 7 for five angles of incidence including 30° ($\phi = 15^\circ, 30^\circ, 45^\circ, 60^\circ, 75^\circ$). The image of a circle $|r_p| = \text{constant}$ in the r_p plane is split into two separate branches in the r_s plane when the condition $|r_p| \leq \tan^2(\phi - 45^\circ)$ is satisfied. This appears in Fig. 7 for the cases of $\phi = 15^\circ$ and $\phi = 75^\circ$. Mirror reflection in the imaginary axis of the orthogonal sets of curves for $\phi = 45^\circ - \theta$ produces the sets that correspond to $\phi = 45^\circ + \theta$. Figure 7 provides useful nomograms for finding r_s for given values of r_p .

V. SIMPLER TRANSFORMATION: MAPPING OF r_s ONTO $\rho = r_p/r_s$

The ratio of reflection coefficients of the p and s polarizations

$$\rho = r_p/r_s \quad (12)$$

is significant because it can be determined experimentally

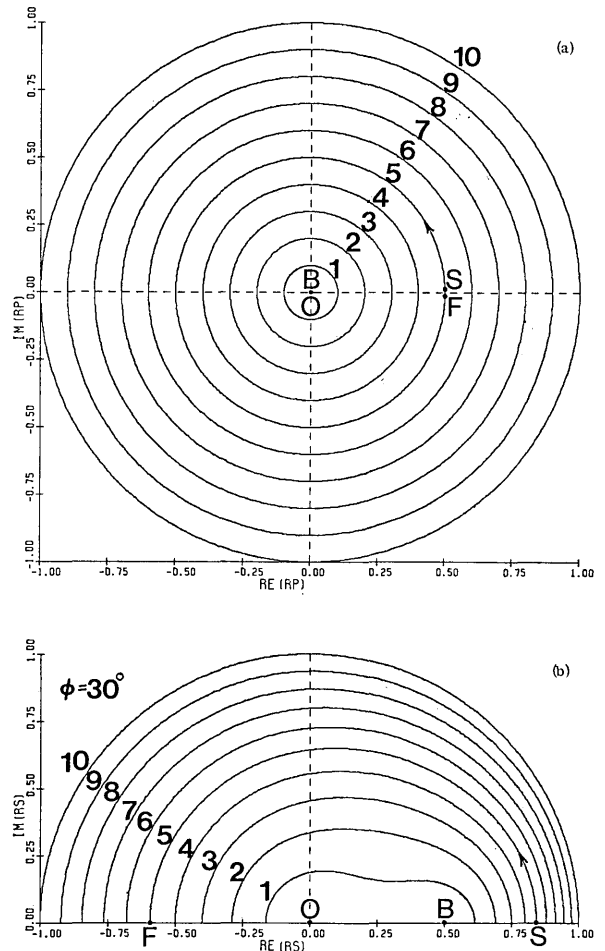


FIG. 6. Inverse mapping of r_p onto r_s according to the complex analytic function $r_s = (1/2) \cos \phi(1 - r_p) + [r_p + (1/4) \cos^2 \phi(1 - r_p)^2]^{1/2}$ when $\phi = 30^\circ$. The equispaced circles centered on the origin 1, 2, 3, ..., 10 in the r_p plane represent lines of equal amplitude reflectance for the p polarization $|r_p| = 0.1, 0.2, 0.3, \dots, 1.0$ respectively and their images in the $|r_s|$ plane are marked by the same numbers.

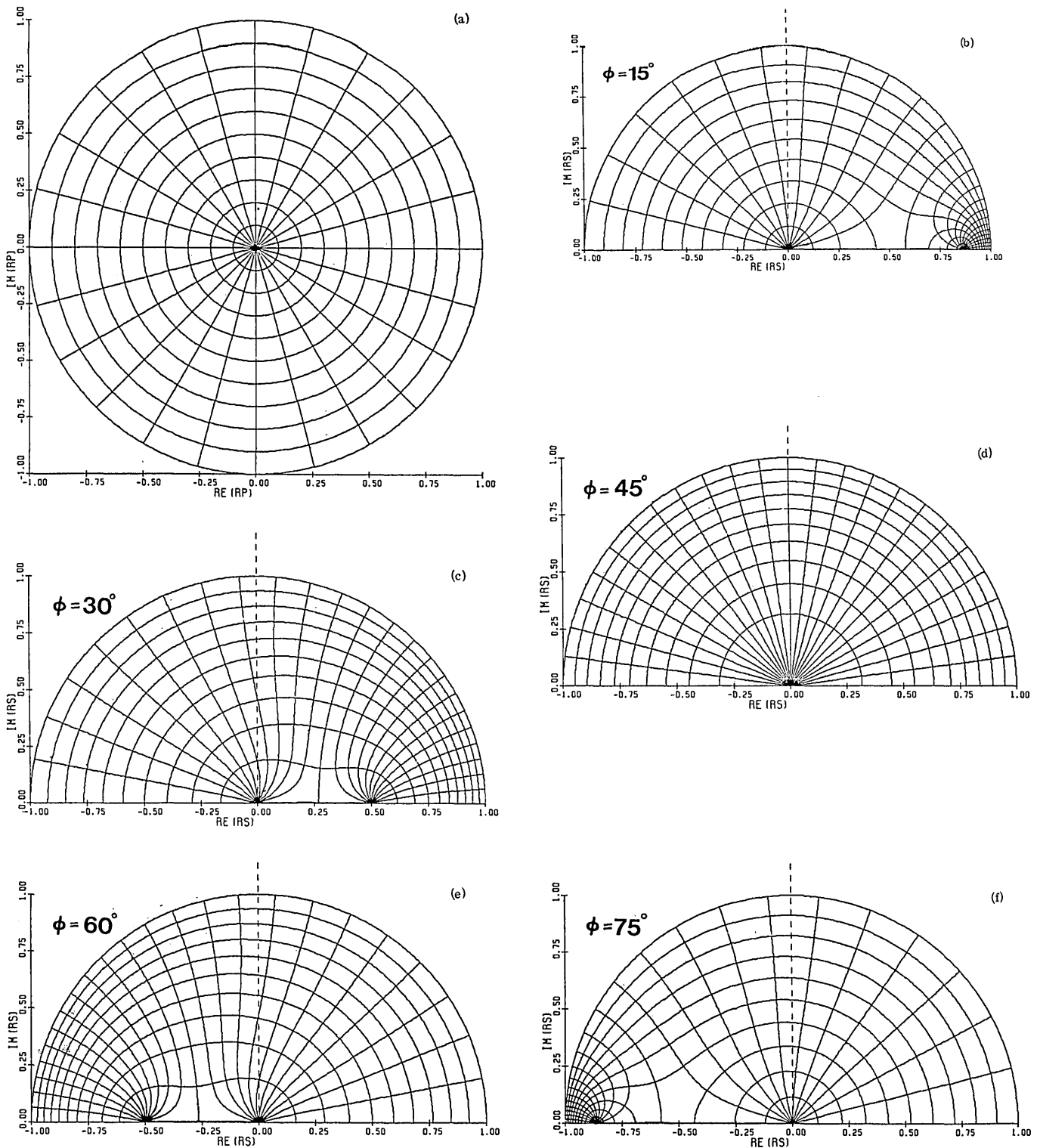


FIG. 7. Inverse mapping of r_p onto r_s according to the complex analytic function $r_s = (\frac{1}{2}) \cos 2\phi(1 - r_p) + [r_p + (\frac{1}{4}) \cos^2 2\phi(1 - r_p)^2]^{1/2}$ when $\phi = 15^\circ, 30^\circ, 45^\circ, 60^\circ, 75^\circ$. The orthogonal families of straight lines and circles through and around the origin in the r_p plane are mapped onto orthogonal sets of curves in the r_s plane. The orthogonal sets that correspond to $\phi = 30^\circ$ are obtained from the superposition of Figs. 5 and 6. To identify individual curves use Figs. 5 and 6 as a guide.

from polarization measurements, i.e. by ellipsometry.¹³ From Eq. (6) we find that

$$\rho = (r_s - \cos 2\phi)/(1 - r_s \cos 2\phi). \quad (13)$$

Equation (13) indicates that ρ is related to r_s via a bilinear

(Möbius) transformation.¹⁰ r_s and ρ are both limited to the upper half of the unit circle in the complex plane.

A bilinear transformation has the distinction of mapping circles (including straight lines which are degenerate circles) in the complex plane of one variable onto circles in the com-

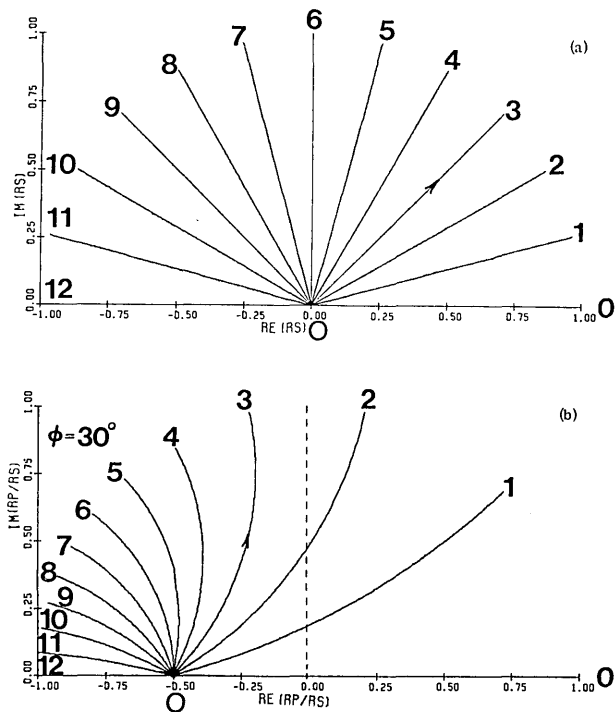


FIG. 8. Mapping of r_s onto $\rho = r_p/r_s$ according to the bilinear transformation $\rho = (r_s - \cos 2\phi)/(1 - r_s \cos 2\phi)$ when $\phi = 30^\circ$. Straight lines through the origin in the r_s plane, $\delta_s = \arg r_s = 0, 15^\circ, 30^\circ, \dots, 180^\circ$, are mapped onto arcs of coaxial circles that pass through the points $\rho = -\cos 2\phi$ and $-\sec 2\phi$ (not shown) in the ρ plane.

plex plane of the other variable. Figure 8 shows how straight lines through the origin of the r_s plane ($\arg r_s = 0, 15^\circ, \dots, 180^\circ$) are mapped onto arcs of coaxial circles in the ρ plane that pass through the common points $\rho = -\cos 2\phi$ inside the unit circle, and $\rho = -\sec 2\phi$ outside the unit circle (not shown in Fig. 8). These two points are the images of $r_s = 0$ and $r_s = \infty$, respectively.

Figure 9 shows the mapping of semicircles centered on the origin of the r_s plane ($|r_s| = 0.1, 0.2, \dots, 1.0$) onto semicircles of coaxial circles in the ρ plane that enclose the point $\rho = -\cos 2\phi$ (which is the image of $r_s = 0$).

The superposition of Figs. 8 and 9 produces orthogonal families of straight lines and semicircles in the r_s plane and orthogonal families of circular arcs and semicircles in the ρ plane. This is shown in Fig. 10 for five angles of incidence including 30° ($\phi = 15^\circ, 30^\circ, 45^\circ, 60^\circ, 75^\circ$). Here also mirror reflection in the imaginary axis relates the orthogonal sets at $\phi = 45^\circ + \theta$ and $45^\circ - \theta$.

The inverse of Eq. (13),

$$r_s = (\rho + \cos 2\phi)/(1 + \rho \cos 2\phi), \quad (14)$$

gives r_s in terms of ρ , also as a bilinear transformation. In a slightly different form Eq. (14) reads

$$r_s = [\rho - \cos 2(90^\circ - \phi)]/[1 - \rho \cos 2(90^\circ - \phi)]. \quad (15)$$

Equation (15) is identical in form with Eq. (13) and is obtained from it by switching the variables r_s and ρ and replacing ϕ by $90^\circ - \phi$. Consequently, Figs. 8–10 describe the inverse transformation $\rho \rightarrow r_s$ if, in these figures, we interchange r_s and ρ and replace ϕ by $90^\circ - \phi$.

VI. REFLECTION PHASE SHIFTS AND DIELECTRIC FUNCTION FROM MEASURED ρ AND s REFLECTANCES AT THE SAME ANGLE OF INCIDENCE

In addition to providing new understanding of the behavior of the fundamental Fresnel reflection coefficients for the p and s polarizations, and also a unified framework for discussion of several specific reflection characteristics, this paper leads to other useful practical results. In particular, we provide simple analytical and graphical methods for determining reflection phase shifts and the dielectric function from measurements of the interface reflectances of the p and s polarizations. This problem has been dealt with before.¹⁴

The interface reflectances are defined by

$$R = |r_l|^2, \quad l = p, s. \quad (16)$$

If we take the squared absolute value of both sides of Eq. (6), we obtain

$$R_p = R_s \frac{R_s + \cos^2 2\phi - 2R_s^{1/2} \cos 2\phi \cos \delta_s}{1 + R_s \cos^2 2\phi - 2R_s^{1/2} \cos 2\phi \cos \delta_s}, \quad (17)$$

where $\delta_s = \arg r_s$ is the reflection phase shift for the s polarization. Equation (17) can be readily solved for δ_s :

$$\cos \delta_s = \frac{(R_s^2 - R_p) + R_s(1 - R_p) \cos^2 2\phi}{2R_s^{1/2}(R_s - R_p) \cos 2\phi}. \quad (18)$$

Equation (18) provides a simple explicit solution for the reflection phase shift δ_s in terms of the intensity reflectances R_p and R_s of the p and s polarizations at the same angle of incidence¹⁵ ϕ . Once δ_s has been found, the complex relative

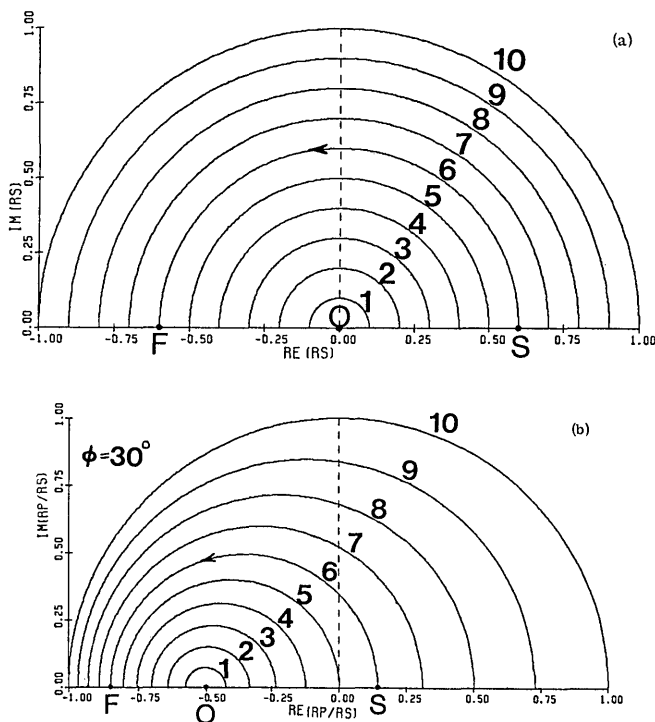


FIG. 9. Mapping of r_s onto $\rho = r_p/r_s$ according to the bilinear transformation $\rho = (r_s - \cos 2\phi)/(1 - r_s \cos 2\phi)$ when $\phi = 30^\circ$. Semicircles centered on the origin in the r_s plane, $|r_s| = 0.1, 0.2, \dots, 1.0$, are mapped onto semicircles of coaxial circles that enclose the point $\rho = \cos 2\phi$ in the ρ plane.

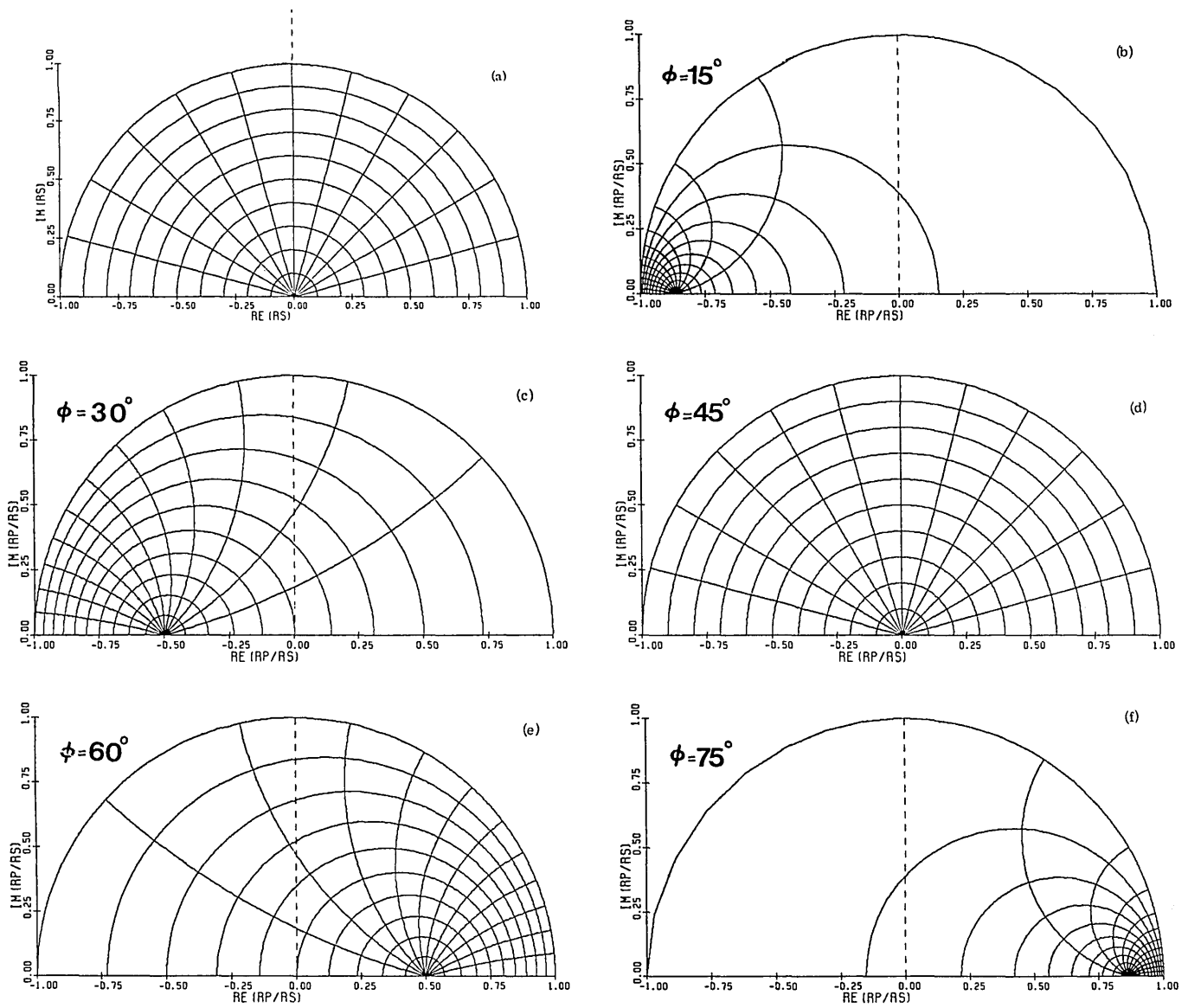


FIG. 10. Mapping of r_s onto $\rho = r_p/r_s$ according to the bilinear transformation $\rho = (r_s - \cos 2\phi)/(1 - r_s \cos 2\phi)$ when $\phi = 15^\circ, 30^\circ, 45^\circ, 60^\circ, 75^\circ$. The orthogonal families of straight lines and semicircles through and around the origin in the r_s are mapped onto orthogonal circle arcs and semicircles through and around the point $\rho = -\cos 2\phi$ in the ρ plane. The orthogonal sets that correspond to $\phi = 30^\circ$ are obtained from the superposition of Figs. 8 and 9. To identify individual curves use Figs. 8 and 9 as a guide.

dielectric function ϵ (the ratio of the dielectric function of the medium of refraction to that of the medium of incidence) can be determined from the now-known complex reflection coefficient $r_s = R_s^{1/2} e^{j\delta_s}$ by

$$\epsilon = \sin^2\phi + \cos^2\phi [(1 - r_s)/(1 + r_s)]^2, \quad (19)$$

which follows directly from Eq. (2).

If we take the argument (angle) of both sides of Eq. (13) or (6), we get

$$\tan\Delta = \frac{R_s^{1/2} \sin\delta_s \sin^2 2\phi}{R_s^{1/2} \cos\delta_s (1 + \cos^2 2\phi) - R_s \cos 2\phi}, \quad (20)$$

where $\Delta = \arg \rho = \delta_p - \delta_s$. Equation (20) gives Δ , hence $\delta_p = \Delta + \delta_s$, after δ_s has been obtained from Eq. (18).

Simple nomograms can be constructed that provide

graphical solutions for δ_s in terms of R_p and R_s . Figure 11 shows one such nomogram in the r_s plane for angle of incidence $\phi = 60^\circ$. It consists of two intersecting sets of semicircles, one centered on the origin representing $|r_s| = \text{constant}$, and the other encircling the point $r_s = \cos 2\phi$ and representing $|\rho| = \text{constant}$. The latter has already been mentioned in connection with Eq. (15). For given values of R_p and R_s we determine $|r_s| = R_s^{1/2}$ and $|\rho| = (R_p/R_s)^{1/2}$ and the point of intersection of the two semicircles that correspond to these values determine the complex reflection coefficient r_s . The angular polar coordinate of the point of intersection is δ_s .

Instead of preprepared nomograms, one can also make one's own graphical construction to determine δ_s from R_p and R_s (or equivalently from $|r_s|$ and $|\rho|$). From Eq. (13) we write

$$|\rho \cos 2\phi| = |r_s - \cos 2\phi|/|r_s - \sec 2\phi|. \quad (21)$$

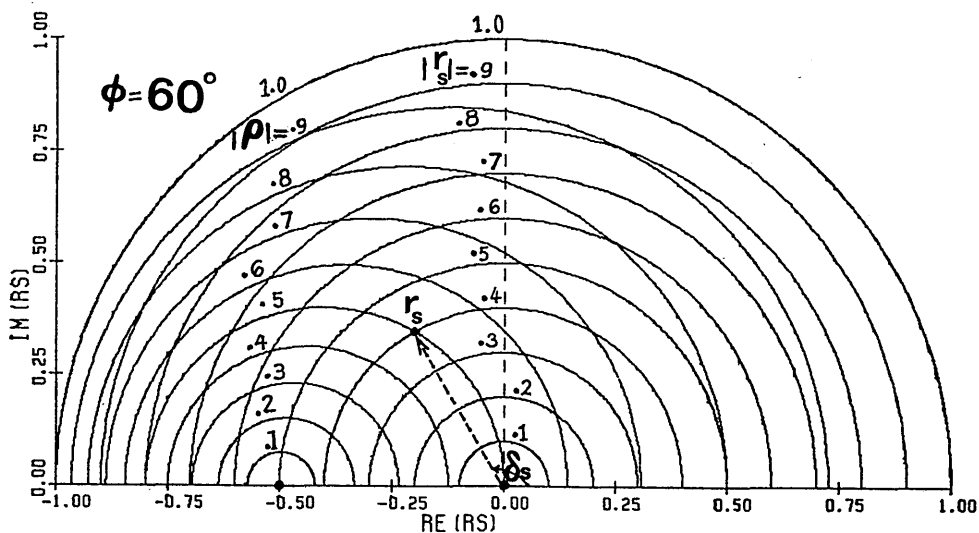


FIG. 11. A nomogram in the complex r_s plane for the graphical determination of the reflection phase shift δ_s from the measured reflectances R_s and R_p of the s and p polarizations at the same angle of incidence $\phi = 60^\circ$. The semicircles centered on the origin represent lines of equal amplitude reflectance for the s polarization $|r_s| = R_s^{1/2} = 0.1, 0.2, 0.3, \dots, 1.0$, while the semicircles that enclose the point $r_s = \cos 2\phi$ represent lines of equal ratio of p and s amplitude reflectances $|\rho| = (R_p/R_s)^{1/2} = 0.1, 0.2, 0.3, \dots, 1.0$. The measured reflectances R_s and R_p specify one semicircle from each family and their point of intersection gives the complex reflection coefficient r_s while its angular polar coordinate gives $\delta_s = \arg r_s$.

According to Eq. (21), the circle in the r_s plane that represents $|\rho|$ equal to a constant is recognized as the locus of a point r_s that has the ratio of its distances to the two fixed points $\cos 2\phi$ and $\sec 2\phi$ on the real axis equal to a constant given by $|\rho| \times |\cos 2\phi|$. The following procedure to graphically determine δ_s becomes evident (see Fig. 12): (i) Mark the points A and B on the real axis at $\cos 2\phi$ (OA) and $\sec 2\phi$ (OB) respectively. (ii) Find the points C and D which internally and externally divide AB in the same ratio $|\rho \cos 2\phi| = (R_p/R_s)^{1/2} |\cos 2\phi|$. (iii) Draw a semicircle with CD as a diameter. (iv) Draw a second semicircle with the origin O as center and of radius $|r_s| = R_s^{1/2}$. (v) The point of intersection of the two semicircles P gives the complex reflection coefficient r_s and its angular polar coordinate gives δ_s .

Similar nomograms and graphical constructions in the complex ρ plane can be used to determine Δ , as the reader can readily verify.

APPENDIX

We will prove that when r_p is real, negative, and in the range

$$-1 \leq r_p \leq -\tan^2(\phi - 45^\circ), \quad (22)$$

r_s becomes complex and its locus, for a given angle of incidence ϕ , is an arc of a circle with center on the real axis at $\sec 2\phi$ and radius of $|\tan 2\phi|$.

It is evident from Eq. (11) that r_s becomes complex when r_p is real only if the quantity under the square root is negative. If we denote such a quality by Q ,

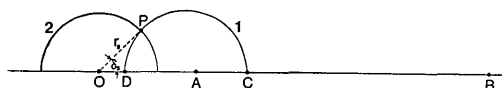


FIG. 12. A graphical construction that can be readily made and used in lieu of the nomogram of Fig. 11.

$$Q = r_p + (1/4) \cos^2 2\phi (1 - r_p)^2, \quad (23)$$

the range of r_p values that make Q negative lies between the roots of the quadratic equation

$$Q = 0. \quad (24)$$

These roots can be put in the form (after some trigonometry)

$$r_p = -(\sec 2\phi \mp \tan 2\phi)^2 = -\tan^2(\phi \mp 45^\circ). \quad (25)$$

Of the range of r_p values between the two roots of Eq. (25), only the subinterval specified by Eq. (22) is physically meaningful because $|r_p| \leq 1$.

With Q negative, Eq. (11) can be rewritten as

$$r_s = x + jy, \quad (26)$$

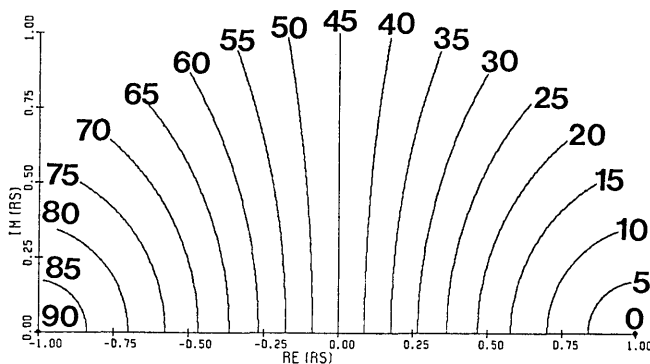


FIG. 13. The loci of the complex reflection coefficient for the s polarization when the reflection coefficient for the p polarization is real and negative in the range $-1 \leq r_p \leq -\tan^2(\phi - 45^\circ)$ at several different angles of incidence $\phi = 0, 5^\circ, 10^\circ, \dots, 90^\circ$ marked by each curve. Each locus or curve at a given ϕ is an arc of a circle with center on the real axis at $\sec 2\phi$ and radius of $|\tan 2\phi|$. Circle arcs that correspond to $\phi = 45^\circ + \theta$ and $45^\circ - \theta$ are mirror images of one another with respect to the imaginary axis which represents $\phi = 45^\circ$.

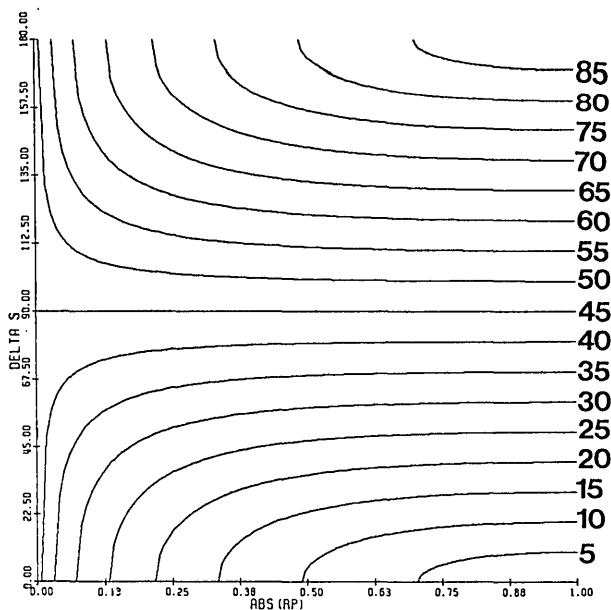


FIG. 14. The reflection phase shift for the s polarization δ_s , when the reflection phase shift for the p polarization δ_p is equal to π , as a function of the absolute value of r_p , with the angle of incidence ϕ as a parameter marked by each curve. Mirror reflection with respect to the line $\delta_s = 90^\circ$, which represents $\phi = 45^\circ$, relate $\delta_s(|r_p|)$ at any pair of angles of incidence $\phi = 45^\circ \pm \theta$.

where

$$x = (1/2) \cos 2\phi (1 - r_p), \quad y = (-Q)^{1/2}. \quad (27)$$

Elimination of r_p between x and y [where Q is given by Eq. (23)] gives

$$(x - \sec 2\phi)^2 + y^2 = \tan^2 2\phi, \quad (28)$$

which is the equation of a circle with center at $(\sec 2\phi, 0)$ and radius of $|\tan 2\phi|$. Of course r_s is restricted to the arc of this circle between the real axis and the upper half of the unit circle. Figure 13 shows the locus of r_s , when r_p is real, negative, and in the range specified by Eq. (22), for angles of incidence ϕ from 5° to 85° in steps of 5° . The limiting cases of $\phi = 0$ and $\phi = 90^\circ$ are represented by the points $r_s = 1$ and $r_s = -1$ respectively.

From Eqs. (26), (27), and (23), we obtain the interesting result $|r_s|^2 = -r_p$, hence

$$|r_s| = |r_p|^{1/2}. \quad (29)$$

Equation (29) indicates that the absolute value of the reflection coefficient (amplitude reflectance) for the s polarization is equal to the square root of that for the p polarization, when

r_p is real negative and r_s is complex. From Eq. (29), the intensity reflectances are interrelated by

$$R_p = R_s^2, \quad (30)$$

a relation that may have been thought before to hold only when the angle of incidence⁵⁻⁷ or the angle of refraction⁹ is 45° .

For completeness, Fig. 14 gives the reflection phase shift $\delta_s = \arg r_s$ as a function of $|r_p|$ for different angles of incidence ϕ from 5° and 85° in steps of 5° .

The results of this appendix complete an earlier analysis¹² in which we proved, starting directly from the equations for the Fresnel coefficients, Eqs. (1) and (2), that r_p can be real while r_s is complex, and in which we also found the conditions that must be satisfied by the dielectric function ϵ for this to happen.

¹See, for example, M. Born and E. Wolf, *Principles of Optics* (Pergamon, New York, 1975), 5th edition, p. 40.

²R. H. Muller, "Definitions and conventions in ellipsometry," *Surf. Sci.* **16**, 14-33 (1969).

³R. M. A. Azzam, "Transformation of Fresnel's interface reflection and transmission coefficients between normal and oblique incidence," *J. Opt. Soc. Am.* **69**, 590-596 (1979).

⁴Equation (6) can be cast in the alternative form $(r_s^2 - r_p)/(r_s - r_s r_p) = \cos 2\phi$. The left-hand-side function of r_s and r_p is therefore real and invariant, at a given angle of incidence ϕ , with respect to changes of media and/or wavelength.

⁵R. M. A. Azzam, "On the reflection of light at 45° angle of incidence," *Opt. Acta* **26** (1979), (in press).

⁶D. W. Berreman, "Simple relation between reflectances of polarized components of a beam when the angle of incidence is 45° ," *J. Opt. Soc. Am.* **56**, 1784 (1966).

⁷S. P. F. Humphreys-Owen, "Comparison of reflection methods for measuring optical constants without polarimetric analysis, and proposal for new methods based on the Brewster angle," *Proc. Phys. Soc. Lond.* **77**, 949-957 (1961).

⁸The second root of the quadratic equation that results from setting the numerator of the right-hand side of Eq. (8) equal to zero has an absolute value greater than 1, hence is physically unacceptable.

⁹R. M. A. Azzam, "Consequences of light reflection at the interface between two transparent media such that the angle of refraction is 45° ," *J. Opt. Soc. Am.* **68**, 1613-1615 (1978).

¹⁰See, for example, A. Kyrala, *Applied Functions of a Complex Variable* (Wiley-Interscience, New York, 1972), Ch. 8.

¹¹The mapping is conformal at all points in the complex plane except where $\partial r_p / \partial r_s = 0$ or ∞ . This excludes the point specified by r_s and r_p in Eqs. (9) and (10).

¹²R. M. A. Azzam, "Reflection of an electromagnetic plane wave with 0 or π phase shift at the surface of an absorbing medium," *J. Opt. Soc. Am.* **69**, 487-488 (1979).

¹³R. M. A. Azzam and N. M. Bashara, *Ellipsometry and polarized Light* (North-Holland, Amsterdam, 1977).

¹⁴M. R. Querry, "Direct solution of the generalized Fresnel reflectance equations," *J. Opt. Soc. Am.* **59**, 876-877 (1969).

¹⁵When $\phi = 45^\circ$, we have $\cos 2\phi = 0$ and $R_p = R_s^2$. This reduces Eq. (18) to $\cos \delta_s = 0/0$, hence δ_s becomes indeterminate, as is expected in this special case.